Spin Injection Into Magnesium Nanowire

Hiroshi Idzuchi[1], Yasuhiro Fukuma[2], Le Wang[2,3], and YoshiChika Otani[1,2,3]

[1]Institute for Solid State Physics, University of Tokyo, Kashiwa 277-8581, Japan
[2]Advanced Science Institute, RIKEN, 2-1 Hirosawa, Wako 351-0198, Japan
[3]Department of Material Physics and Chemistry, University of Science and Technology Beijing, Beijing 100083, China

Spin injection into magnesium from Permalloy is performed in the lateral spin valve geometry. A large spin valve signal of 3.1 $\mathrm{m}\Omega$ is observed at room temperature. The injector-detector separation dependence of the spin valve signal is analyzed by using a one-dimensional spin-diffusion model. The analysis yields the spin diffusion length of about 200 nm for the Mg nanowires. The short spin diffusion length of magnesium which has a small spin-orbit interaction can possibly be explained by considering the spin-hot-spot relaxation mechanism proposed by Fabian and Das Sarma.

***Index Terms*—Lateral spin valve, spin hot spot, spin injection, spin relaxation.**

I. Introduction

SPINTRONICS has drawn great attention in recent years because of the novel device functionalities derived from both electronic charge and spin. The injection, manipulation and detection of spin currents are indispensable for developing the spintronic devices.

The pioneer work on electrical spin injection and detection had been carried out by Johnson and Silsbee [1]. Then Jedema *et al.* demonstrated non-local lateral spin valve measurements [2], which brought renewed interests in the lateral spin valves in response to the timely development in both micro-fabrication technology and emergent interest in spintronics. The non-local spin injection in the lateral spin valves provides an effective method to generate a pure spin current, i.e. a diffusive flow of spin angular momentum accompanied by no flow of charge. This enables us to study a spin transport and relaxation mechanism in the nonmagnetic nanowire without a spurious effect of charge current.

The spin relaxation in nonmagnetic metals is caused by the Elliot-Yafet mechanism [3], [4] where admixture of the opposite spin states due to spin-orbit interaction causes spin-flip via phonon and impurity scatterings. Light metal Mg, having a weak spin-orbit interaction, is thus a promising candidate for materials with longer spin diffusion length. Recently, we have reported the primary experimental results on the lateral spin valves with Permalloy (Py)/Mg junctions [5]. Here, we further discuss spin injection and spin transport in the Mg nanowires in detail.

II. Experimental Methods

Lateral spin valve (LSV) devices are fabricated by means of shadow evaporation combined with e-beam lithography using a suspended resist mask, consisting of a bilayer resist

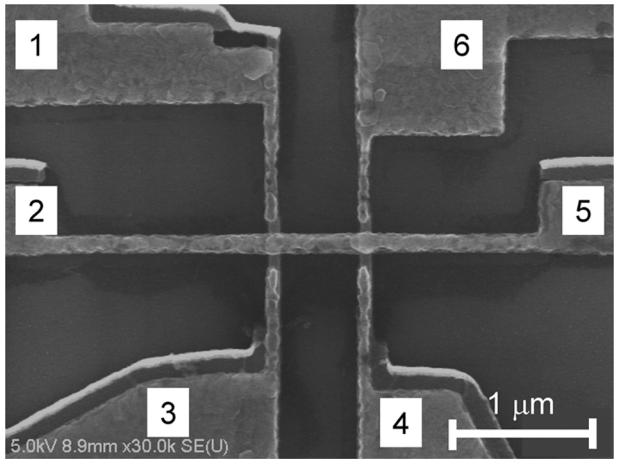

Fig. 1. Scanning electron microscope (SEM) image of fabricated lateral spin valve device.

500-nm-thick Methyl methacrylate (MMA) and 50-nm-thick Poly methyl methacrylate (PMMA) formed on $\mathrm{Si}/\mathrm{SiO}_2$ substrates. The sensitivity of MMA is higher than that of PMMA and thereby undercut structure is created after development. Firstly a Py layer is e-beam deposited at an angle of 45 degrees from substrate normal. Then, the substrate is transferred under vacuum to the different chamber with a base pressure 5×10^{-10} Torr, and a Mg layer is e-beam deposited normal to the substrate cooled by liquid nitrogen. Finally, a 5-nm-thick MgO capping layer is deposited to protect the surface. After a lift-off procedure, the structure is examined by means of scanning electron microscopy (SEM), as shown in Fig. 1. Three classes of devices, LSV1, 2, and 3, with different Py and Mg wire widths are prepared. For LSV1, a Py wire with the width w_{Py} of 80 nm is bridged by a Mg wire with w_{Mg} of 110 nm. For LSV2 and 3, the values of w_{py} are different, 80 nm for LSV2 and 130 nm for LSV3 while the Mg wire width w_{Mg} is set at 170 nm. The thicknesses of all the Py and Mg layers are 20 and 100 nm, respectively. The center-to-center separation d between the Py injector and detector is varied from 250 nm to 800 nm. After examination of SEM, all the devices are covered with a 10-nm-thick sputter deposited SiO_2 layer to prevent oxidation of the side edges of Mg wires.

Manuscript received September 27, 2010; revised January 11, 2011; accepted January 13, 2011. Date of current version May 25, 2011. Corresponding author: H. Idzuchi (e-mail: idzuchi@issp.u-tokyo.ac.jp).

Color versions of one or more of the figures in this paper are available online at http://ieeexplore.ieee.org.

Digital Object Identifier 10.1109/TMAG.2011.2108272

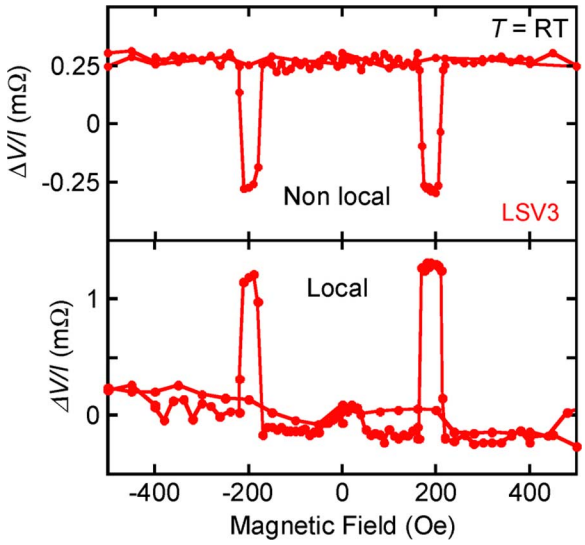

Fig. 2. Field dependence of nonlocal and local spin valve signals at room temperature for device with injector-detector separation of 400 nm.

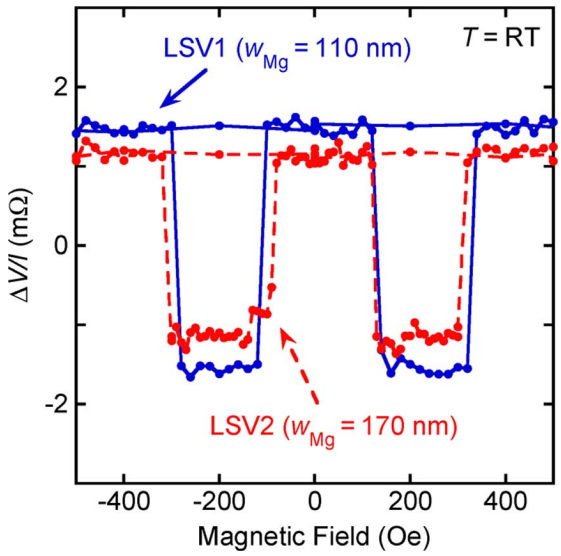

Fig. 3. Field dependence of nonlocal spin valve signal at room temperature for devices with different Mg wire widths and injector-detector separation of 250 nm.

Spin transport measurements are performed for both nonlocal and local configurations at room temperature (RT). For the nonlocal measurements as in Fig. 1, the current is applied between terminals 4 and 5 and the voltage is detected by using terminals 2 and 3. For the local measurements, the current is applied between terminals 3 and 4 and then the voltage is detected by using terminals 1 and 6. We use current-bias lock-in technique with an amplitude of 0.20 mA and a frequency of 79 Hz. The magnetic field is applied along the easy axis of the Py wires.

III. Results and Discussions

Fig. 2 shows the field dependence of the nonlocal and local spin valve signals for LSV3 with $d = 400$ nm. Clear switching behavior is observed for the nonlocal and local measurements. The switching field of the Py wire is controlled by setting different domain-wall nucleation field, i.e., the injector has a large domain wall reservoir at the edge of the wire, producing lower nucleation field than that of the detector. Spin valve signal $\Delta R_{\rm S} = (V_{\rm P} - V_{\rm AP})/I$, is defined as the overall signal change between parallel and antiparallel configurations of the two Py wires. As can be seen in Fig. 2, $\Delta R_{\rm S} = 1.2$ mΩ for the local spin valve measurement is 2.4 times larger than that of 0.5 mΩ for the nonlocal spin valve measurement, which is in reasonable agreement with the factor of 2 expected in [6].

A one-dimensional spin diffusion model predicts that $\Delta R_{\rm S}$ is inversely proportional to the Py/Mg junction area $w_{\rm Py}w_{\rm Mg}$ [6]–[8]. We therefore fabricated LSVs with different $w_{\rm Mg}$. Fig. 3 shows the spin valve signal of LSV1 and LSV2 with $d = 250$ nm. $\Delta R_{\rm S}$ is increased from 2.4 mΩ to 3.1 mΩ by reducing $w_{\rm Mg}$. The junction resistance is measured by a typical four-probe measurement where the current is applied between terminals 4 and 5 and the voltage is detected by using terminals 6 and 2. The junction resistance is below the resolution ability of 1 fΩm^2 of our measurement system. We thus assume the Py/Mg junction is transparent, i.e., zero interface resistance. The $\Delta R_{\rm S}$ of our LSVs with the Py/Mg junctions is much larger than that of LSVs with other transparent ohmic junctions such as Py/Cu, Py/Ag, Py/Al, Co/Cu and Co/Al [2], [6], [9]–[12].

Fig. 4 shows $\Delta R_{\rm S}$ as a function of d for various LSVs. $\Delta R_{\rm S}$ decreases with increasing d due to a spin-flip scattering during the diffusive spin transport in the Mg nanowire. $\Delta R_{\rm S}$ can be given as a solution of the one-dimensional spin dependent diffusion equation [7]. Assuming the transparent contact between Py and Mg, the $\Delta R_{\rm S}$ is expressed as

$$\Delta R_S = 2R_{SN}\frac{\left(P_F\frac{R_{SF}}{R_{SN}}\right)^2 e^{-\frac{d}{\lambda_N}}}{\left(1+2\frac{R_{SF}}{R_{SN}}\right)^2 - e^{-\frac{2d}{\lambda_N}}} \quad (1)$$

where $P_{\rm F}$ is the spin polarization of Py. $R_{\rm SN} = 2\rho_{\rm N}\lambda_{\rm N}/t_{\rm N}w_{\rm N}$ and $R_{\rm SF} = 2\rho_{\rm F}\lambda_{\rm F}/w_{\rm F}w_{\rm N}/(1-P_{\rm F}^2)$ are the spin resistance for Mg and Py, respectively, where ρ the resistivity, λ the spin diffusion length, t the thickness, and w the width. The subscripts of F and N represent Py and Mg, respectively.

The experimental results are fitted to (1) by adjusting parameters $P_{\rm F}$ and $\lambda_{\rm N}$. The value of $\rho_{\rm F}$ is 4.7×10^{-7} Ωm and the values of $\rho_{\rm N}$ for $w_{\rm Mg} = 170$ nm and 110 nm are 1.0×10^{-7} and 1.5×10^{-7} Ωm, respectively. The reported value of $\lambda_{\rm F} = 5$ nm is used for Py [13]. The deduced fit parameters are $P_{\rm F} = 0.30 \pm 0.07$ and $\lambda_{\rm N} = 175 \pm 45$ nm for LSV1, $P_{\rm F} = 0.27 \pm 0.03$ and $\lambda_{\rm N} = 210 \pm 30$ nm for LSV2, and $P_{\rm F} = 0.33 \pm 0.03$ and $\lambda_{\rm N} = 230 \pm 30$ nm for LSV3. The shorter $\lambda_{\rm N}$ for the narrower Mg wire could be due to impurity and defect scatterings. The value of $P_{\rm F}$ is relatively high in LSVs, indicating a good quality of the Py/Mg interface. $\lambda_{\rm N}$ of Mg shows a similar value reported for Ag, Cu and Al [14]. Mg is a lighter element than those reported for LSVs, implying smaller spin-orbit interaction. However, the obtained $\lambda_{\rm N}$ of Mg is a few hundred nanometers at RT.

To discuss the origin, we focus on the spin-flip mechanism in the nonmagnetic metal. Monod reported that the spin relaxation in metals is divided into two groups: one is the monovalent alkali

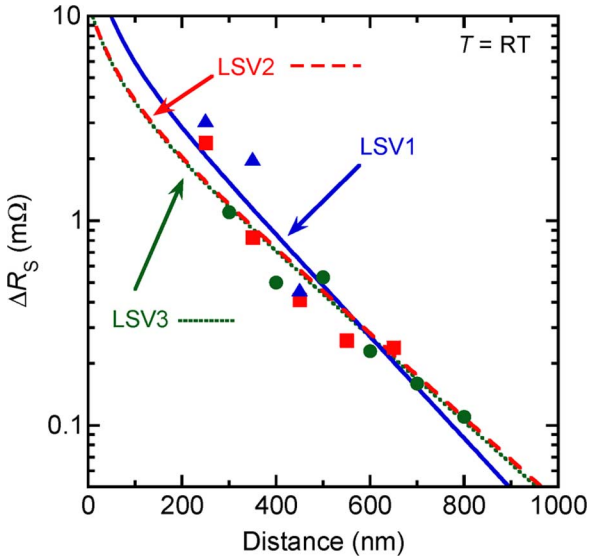

Fig. 4. Injector-detector separation dependence of nonlocal spin valve signal $\Delta R_{\rm S}$ for devices with different Mg and Py wire widths. Lines are fitted curves using eq. (1).

and noble metals, and the other is the polyvalent metals such as Al and Mg [15]. The former group shows a universal curve in the $1/\{\tau_{\rm sf}^{\rm ph}(\lambda_{\rm SOI}/\Delta E)^2\}$ vs $T/T_{\rm D}$ plot, where $\tau_{\rm sf}^{\rm ph}$ the spin-flip time from phonon, $\lambda_{\rm SOI}$ spin-orbit splitting, ΔE the energy distance between the band state in question and the state which produces largest spin-orbit pertubation, and $T_{\rm D}$ the Debye temperature. The latter group has much shorter $\tau_{\rm sf}^{\rm ph}$ than for the monovalent metals because a complicated Fermi surface enhances a spin-flip scattering [16]. The total spin-flip time $\tau_{\rm sf} = \lambda_N^2/D$, is deduced from $\lambda_{\rm N}$ determined by the injector-detector separation dependence of $\Delta R_{\rm S}$. D is the diffusion constant, which is determined by Einstein relation $\rho_{\rm N}^{-1} = e^2 DN(\varepsilon_{\rm F})$, where $N(\varepsilon_{\rm F}) = 1.88 \times 10^{22}\ {\rm states/eV/cm^3}$ is the density of state on the Fermi energy in Mg [17]. $\tau_{\rm sf}$ of 14 ps, 13 ps and 16 ps are obtained for the Mg nanowire in LSV1, LSV2 and LSV3, respectively.

We compare the obtained $\tau_{\rm sf}$ with that of Na because the band parameters are similar to each other, e.g., the normalizing factor $(\lambda_{\rm SOI}/\Delta E)^2$ is 1.32×10^{-5} and 2.73×10^{-5} for Mg and Na, respectively [15]. $\tau_{\rm sf}$ of the Mg nanowire is 14 ps at room temperature which is close to $T_{\rm D} = 290$ K, and $\tau_{\rm sf}$ of Na is 20 ns at $T_{\rm D} = 150$ K [18]. The total $\tau_{\rm sf}$ is expressed as

$$\frac{1}{\tau_{\rm sf}} = \frac{1}{\tau_{\rm sf}^{\rm ph}} + \frac{1}{\tau_{\rm sf}^{\rm imp}} \tag{2}$$

where $\tau_{\rm sf}^{\rm imp}$ is the spin-flip time from impurities. According to the Elliott-Yafet mechanism, each spin-flip process is proportional to each momentum relaxation time for the phonon and impurity scatterings [19]:

$$\frac{1}{\tau_{\rm sf}} = \frac{\varepsilon_{\rm ph}}{\tau_e^{\rm ph}} + \frac{\varepsilon_{\rm imp}}{\tau_e^{\rm imp}} \propto \varepsilon_{\rm ph}\rho_{\rm ph} + \varepsilon_{\rm imp}\rho_{\rm imp} \tag{3}$$

where $\tau_e^{\rm ph}$ and $\tau_e^{\rm imp}$ are momentum relaxation time from phonon and impurity scatterings, respectively, and $\varepsilon_{\rm ph}$ and $\varepsilon_{\rm imp}$ are the spin-flip probability for the each momentum relaxation time. $\rho_{\rm ph}$ and $\rho_{\rm imp}$ are respectively the phonon and impurity contributions. In order to estimate $\tau_{\rm sf}^{\rm ph}$ of the Mg nanowire, the residual resistivity ratio (RRR) was measured. The ${\rm RRR} \sim 2.5$ yields $\tau_{\rm sf}^{\rm ph} \sim 42$ ps by using (2) and (3) with assuming $\varepsilon_{\rm imp} \sim 3\varepsilon_{\rm ph}$ [6]. For bulk Na, $\tau_{\rm sf}^{\rm ph}$ is estimated to be 20 ns because of ${\rm RRR} \sim 7000$. $\tau_{\rm sf}^{\rm ph}$ of the Mg nanowire is three orders of magnitude shorter than that of Na. Such a significant reduction of $\tau_{\rm sf}^{\rm ph}$ for Mg could not explain by the simple Elliott-Yafet mechanism. Fabian and Das Sarma reported that polyvalent metals such as Al and Mg have a complex Fermi surfaces which cross Brillouin zone boundaries, causing accidental degeneracy points between majority and minority spin bands [16]. This strongly enhances the spin relaxation in Mg.

IV. Conclusion

Spin injection into Mg nanowires is performed by using Py/Mg lateral spin valves at room temperature. Nonlocal and local spin valve signals show the same switching characteristics and the amplitude of the local spin valve signal is 2.4 times larger than that of the nonlocal spin valve signal. These facts assure that one-dimensional spin diffusion model is applicable to explain the observed spin valve behaviors in the Py/Mg devices. Large nonlocal spin valve signal of 3.1 $\rm m\Omega$ is measured in LSVs with the 110 nm-wide Mg wires. The analyses of the experimental data using the one-dimensional spin diffusion model yield the spin diffusion length of a few hundred nanometers for the Mg nanowires. The short spin diffusion length anticipates the existence of spin-hot-spot and the estimated spin-flip time of about 14 ps is consistent with the theoretical prediction by Fabian and Das Sarma: the spin-flip time of Mg is about three orders of magnitude shorter than that of monovalent metals with similar band structure [16].

Acknowledgment

This work was supported in part by a Grant-in-Aid for Scientific Research on Priority Area "Creation and control of spin current" (No. 19048013) from the Ministry of Education, Culture, Sports, Science and Technology, Japan.

References

[1] M. Johnson and R. H. Silsbee, "Interfacial charge-spin coupling: Injection and detection of spin magnetization in metals," *Phys. Rev. Lett.*, vol. 55, pp. 1790–1793, 1985.

[2] F. J. Jedema, A. T. Filip, and W. B. Van, "Electrical spin injection and accumulation at room temperature in an all-metal mesoscopic spin valve," *Nature*, vol. 410, pp. 345–348, 2001.

[3] R. J. Elliott, "Theory of the effect of spin-orbit coupling on magnetic resonance in some semiconductors," *Phys. Rev.*, vol. 96, pp. 266–279, 1954.

[4] Y. Yafet, "G-factors and spin-lattice relaxation of conduction electrons," *Solid State Physics*, vol. 14, pp. 1–98, 1963.

[5] H. Idzuchi, Y. Fukuma, L. Wang, and Y. Otani, "Spin diffusion characteristics in magnesium nanowires," *Appl. Phys. Exp.*, vol. 3, p. 063002, 2010.

[6] F. J. Jedema, M. S. Nijboer, A. T. Filip, and W. B. van, "Spin injection and spin accumulation in all-metal mesoscopic spin valves," *Phys. Rev. B*, vol. 67, p. 085319, 2003.

[7] S. Takahashi and S. Maekawa, "Spin injection and detection in magnetic nanostructures," *Phys. Rev. B*, vol. 67, p. 052409, 2003.
[8] T. Kimura, Y. Otani, and J. Hamrle, "Enhancement of spin accumulation in a nonmagnetic layer by reducing junction size," *Phys. Rev. B*, vol. 73, p. 132405, 2006.
[9] T. Kimura, T. Sato, and Y. Otani, "Temperature evolution of spin relaxation in a NiFe/Cu lateral spin valve," *Phys. Rev. Lett.*, vol. 100, p. 66602, 2008.
[10] T. Kimura and Y. Otani, "Large spin accumulation in a permalloy-silver lateral spin valve," *Phys. Rev. Lett.*, vol. 99, p. 196604, 2007.
[11] Y. Fukuma, L. Wang, H. Idzuchi, and Y. Otani, "Enhanced spin accumulation obtained by inserting low-resistance MgO interface in metallic lateral spin valves," *Appl. Phys. Lett.*, vol. 97, p. 012507, 2010.
[12] Y. Ji, A. Hoffmann, J. E. Pearson, and S. D. Bader, "Enhanced spin injection polarization in Co/Cu/Co nonlocal lateral spin valves," *Appl. Phys. Lett.*, vol. 88, p. 052509, 2006.
[13] S. Dubois, L. Piraux, J. M. George, K. Ounadjela, J. L. Duvail, and A. Fert, "Evidence for a short spin diffusion length in permalloy from the giant magnetoresistance of multilayered nanowires," *Phys. Rev. B*, vol. 60, pp. 477–484, 1999.
[14] J. Bass and W. P. Pratt, "Spin-diffusion lengths in metals and alloys, and spin-flipping at metal/metal interfaces: An experimentalist's critical review," *J. Phys. Condens Matter*, vol. 19, p. 183201, 2007.
[15] P. Monod and F. Beuneu, "Conduction-electron spin flip by phonons in metals: Analysis of experimental data," *Phys. Rev. B*, vol. 19, pp. 911–914, 1979.
[16] J. Fabian and S. Das Sarma, "Spin relaxation of conduction electrons in polyvalent metals: Theory and a realistic calculation," *Phys. Rev. Lett.*, vol. 81, pp. 5624–5627, 1998.
[17] D. A. Papaconstantopoulos, *Handbook of the Band Structure of Elemental Solids*. New York: Plenum, 1986, pp. 57–59.
[18] F. Vescial, N. S. VanderVen, and R. T. Schumacher, "Spin-lattice relaxation time of conduction electrons in sodium metal," *Phys. Rev.*, vol. 134, pp. A1286–A1289, 1964.
[19] G. Mihajlović, J. E. Pearson, S. D. Bader, and A. Hoffmann, "Surface spin flip probability of mesoscopic Ag wires," *Phys. Rev. Lett.*, vol. 104, p. 237202, 2010.